Al_3H stable and transition state structures

Nick Gonzales and Jack Simons
Chemistry Department, University of Utah, Salt Lake City, Utah 84112

(Received 11 July 1994; accepted 14 September 1994)

In this study we predict, based on our multiconfigurational and higher level correlated *ab initio* electronic structure calculations, the geometries and relative energies of the Al_3H and Al_3 molecules. We found three minima on the Al_3H potential energy surface, two of which are nearly energetically degenerate: a C_{2v} σ-bonded structure and a C_{3v} π-bonded structure. Two Al_3H transition states were also found: one that connects the C_{3v} and C_{2v} minima and another that connects one C_{3v} minimum to another C_{3v} minimum. We also predict the lowest Al_3 electronic state to be the $^2A_1'$ state which has the valence orbital occupation of $(a_1')^2(e')^4(a_2'')^2(a_1')^1$. © *1994 American Institute of Physics.*

I. INTRODUCTION

Small atomic clusters have been the focus of much experimental and theoretical research in the past decade.[1] Clusters of lighter alkali atoms and alkaline earth atoms were among the first to be studied theoretically using *ab initio* methods because they are computationally tractable, having relatively few valence electrons although possessing four valence orbitals per atom.[2] Even the smallest such clusters present significant computational challenge due to the relatively large number of low-energy electronic states and because of state degeneracies and surface intersections that occur for symmetrical nuclear arrangements. For example, degenerate electronic states of alkali trimers display classic first-order Jahn–Teller (FOJT) distortions causing D_{3h} symmetry structures to evolve into C_{2v} symmetry.[3]

In the present work, we examine a small cluster of group III atoms for which the density of low-lying electronic states is even higher. Earlier work[4] from this group began this study by considering the B_3 molecule and its bonding to H atoms.[5] Here, we extend this study to Al_3 and Al_3H.

A. The B_3 cluster

Clusters of group III elements produce a high density of low-lying electronic states because each atom contributes three valence electrons and four valence orbitals. Unlike the alkali trimers, the boron trimer whose higher occupied valence molecular orbitals (MOs) and valence MO occupations for the two lowest energy $^2A_1'$ and $^2A_2''$ states are shown in Fig. 1, is not susceptible to first-order Jahn–Teller distortions in its equilateral triangular $^2A_1'$ ground state. However, there is a low lying $^4E''$ excited state, whose valence MO occupancy is depicted in Fig. 2, that FOJT distorts to produce $^4B_1$ and $^4A_2$ states of C_{2v} symmetry.[4] In Figs. 1 and 2 only the three σ bonding, one π bonding, and three nonbonding valence orbitals are shown. The other five π^* and σ^* valence orbitals are higher in energy and are not shown.

In an earlier paper, Hernandez and Simons[4] showed that as the two $^4E''$ states of the boron trimer Jahn–Teller distort and evolve along a C_{2v}-constrained path, one state ($^4A_2$) drops in energy and becomes a geometrical minimum while the other state ($^4B_1$) increases in energy to produce a first-order transition state that is geometrically unstable along a vibrational mode of b_2 symmetry. The lower-energy surface has three equivalent minima connected by three equivalent transition states as shown in Fig. 2(b). The higher energy surface also has three equivalent minima connected by three equivalent transition states.

A primary motivation for studying the boron trimer was to characterize the large number of low lying electronic states (e.g., within 7000 cm^{-1} of the ground state there are 11 electronic states) and to characterize the spin and spatial symmetry of the ground state to assist in interpreting ESR experimental data.[6]

B. The Al_3 cluster

In the early stages of the present work, we examined the valence states of the aluminum trimer whose corresponding

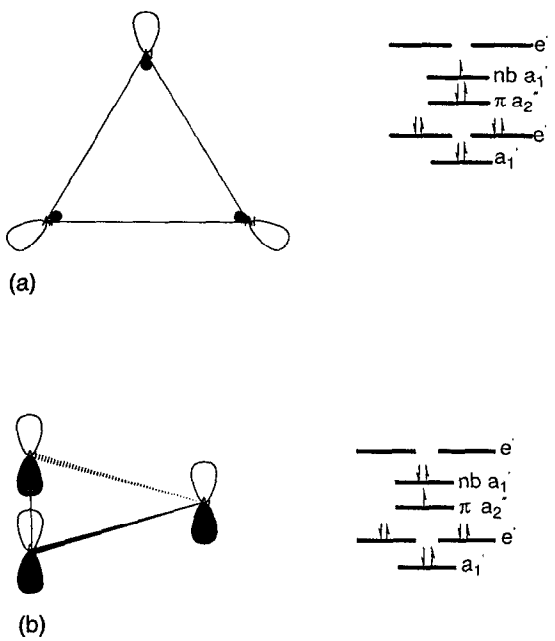

FIG. 1. (a) Valence nonbonding orbital of A_1' symmetry and orbital occupation of the $^2A_1'$ states of B_3 and Al_3. (b) Valence π-type orbital of A_2'' symmetry and orbital occupation of the $^2A_2''$ states of B_3 and Al_3.

 0021-9606/94/101(12)/10746/7/$6.00

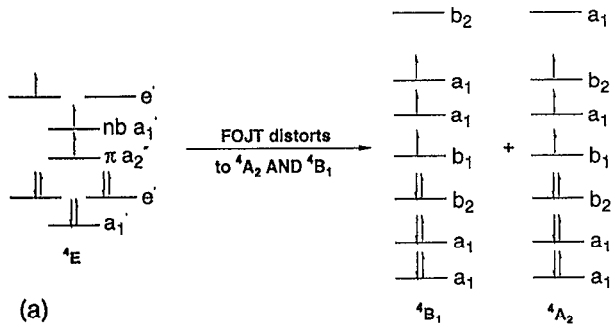

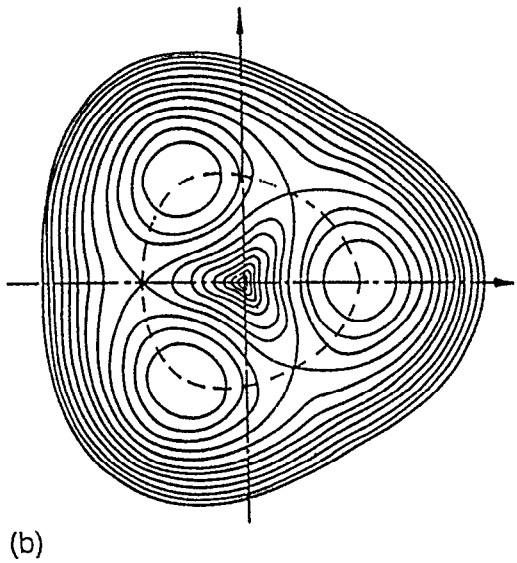

FIG. 2. (a) First order Jahn–Teller distortion of the $^4E''$ state. (b) Three equivalent C_{2v} minima on the $^4A_2$ surface of B_3.

states were studied in the earlier B_3 work. We anticipated that the molecular orbitals in Al_3 would be split less strongly into bonding and antibonding combinations than in B_3, so the density of states would be even higher than in B_3.

Experimentally, the ground state of the aluminum trimer is known to have a magnetic moment consistent with a doublet spin state.[7] The latest ESR analysis of Al_3 by Weltner and co-workers[6] shows that the trimer ground state has a doublet spin state and an equilateral geometry (i.e., three equivalent Al centers). Weltner also found an appreciable amount of s character in the ground state wave function (8%), which precludes the $^2A_2''$ state [see Fig. 1(b)] because its unpaired spin density resides in a π-type orbital that is odd under the molecular σ_h plane and hence, contains no s character. Both experiments thus suggest that the trimer ground state is of $^2A_1'$ symmetry.

However, experiment and theory are difficult to reconcile in this case because the near degeneracy of the two sets of states in the doublet ($^2A_1'$ and $^2A_2''$) and quartet ($^4B_1$ and $^4A_2$) manifolds complicates an accurate prediction of the electronic ground state.[8] For example, even the extensive CI calculations by Baucshlicher and co-workers[9] predict the $^4A_2$ state [Fig. 2(a)] to lie slightly below the $^4B_1$ [Fig. 2(a)] and $^2A_1'$ [Fig. 1(a)] states with the $^2A_2''$ [Fig. 1(b)] state being highest. In contrast, our calculations (perhaps fortuitously) predict an order consistent with Weltner's experimental findings and with the earlier theoretical work of Tse.[8(a)]

Although the aluminum trimer has been studied both by experiment[10] and theory,[8,9] the bonding of Al_3 with even simple radicals such as H atoms has not. Since aluminum has the same number of valence electrons as boron, one would expect similarities in the $H+B_3 \rightarrow B_3H$ and $H+Al_3 \rightarrow Al_3H$ reactions and in the structures of the B_3H and Al_3H hydrides. Electron deficient three-center two-electron bonding might occur in Al_3H since aluminum is also orbitally rich and electron poor, although boron is, of course, expected to display a greater propensity for such bonding. Our findings on these questions are treated in Sec. III after our computational tools are described in Sec. II.

TABLE I. Calibration of Al atomic bases using IP, EA, and $^2P \rightarrow {}^4P$ excitation energies (kcal/mol).

Basis	No. of contracted basis functions	IP	EA	^4P
Ahlrichs (Ref. 13)	32[a]	131.6	1.6	77.8
D-VTZ (Ref. 14)	27[a]	136.9	9.1	66.8
HW-ECP (Ref. 12)	18[a]	132.8	1.4	76.4
6-311+G* (Ref. 15)	31	131.8	2.5	77.5
aug-cc-p VDZ (Ref. 11)	29	135.5	8.7	79.0
Experiment		138.0 (Ref.18)	10.6 (Ref.19)	83.0 (Ref.18)

[a]These bases have a diffuse s function, a diffuse p function, and a d polarization function added to the valence basis.

II. COMPUTATIONAL DETAILS

A. Orbital basis set

After extensive basis set testing, we decided to use Dunning's augmented correlation-consistent polarized valence double-zeta (aug-cc-pVDZ)[11] bases for the hydrogen and aluminum atoms. The adequacy of the basis was judged by how well it reproduced various atomic properties such as the ionization potential IP, the electron affinity EA, and low-energy (i.e., $3s^23p^1 \rightarrow 3s^13p^2$ for Al) excitation energies. Several other basis sets such as the valence basis associated with the effective core potential (ECP) of Hay and Wadt,[12] a $(12s9p/7s5p)$ basis by Ahlrichs and co-workers,[13] Dunning's valence triple zeta,[14] and Pople's[15] 6-311+G* basis were also tested but they did not reproduce the Al atomic properties as well as the basis we chose to employ (see Table I). Because the states of Al_3 and Al_3H of interest here are expected to contain significant Al^+ or Al^- character or character derived from $s^2p^1 \rightarrow s^1p^2$ configurations, we were required to choose a basis set that produced IP, EA, and $^2P \rightarrow {}^4P$ excitation energies all in reasonable agreement with known experimental data. As seen from the data of Table I, only the aug-cc-pVDZ basis came close to experiment for all three energies.

B. Choice of electronic configurations

1. CAS MCSCF level geometry optimization

In forming a set of electronic configurations to use in examining the myriad of low-energy valence states in Al_3, we specify a set of orbitals that are doubly occupied in all configuration state functions (CSFs) as well as a set of valence orbitals among which the specified valence electrons are distributed. If the valence electrons are distributed in all possible ways consistent with the overall spin and spatial symmetry of the state of interest, one forms the set of complete active space (CAS) CSFs. The amplitudes of the CSFs and the expansion coefficients of the MOs are determined by the multi-configurational-self-consistent-field (MCSCF) approach. This process is especially useful when several states of similar energy are anticipated and when several different arrangements of the molecular framework are to be studied, as in the present study where two nearly degenerate states of Al_3, multiple Al_3H structures, and several transition states connecting these structures are analyzed.

The choice of active valence orbitals for use in constructing our CSFs was guided by the following requirements:

(a) The CSF space must be flexible enough to properly describe at least the nondynamical correlation effects on the two lowest states (i.e., the $^2A_1'$ and $^2A_2''$ radical states) of the aluminum trimer because it is to these states that the states of Al_3H correlate at large interfragment distances.

(b) The CAS wave function should be capable of dissociating properly into the aluminum trimer and a hydrogen atom.

(c) The active orbitals should include those derived from the H $1s$ and Al $3s$ and $3p$ atomic orbitals.

These conditions force one to include the three Al–Al σ-bonding orbitals, the delocalized Al bonding π orbital, the three nonbonding Al based n orbitals, and the other five linear combinations of the aluminum $3s$ and $3p$ atomic orbitals for correlation as well as the $1s$ orbital of the H atom. The $1s$, $2s$, and $2p$ atomic orbitals of the aluminum atoms are core orbitals that are doubly occupied in all CSFs. We include all 10 valence electrons in our MCSCF wave function. For Al_3H, the resulting CAS space involving thirteen active orbitals with their ten active electrons gave rise to 429 000 total CSFs of $^1A_1$ symmetry. This number of CSFs was prohibitive for us to use in exhaustively searching the six-dimensional geometry space. To reduce the number of CSFs beyond those contained in the full CAS space, we first examined the closed-shell SCF function which places the ten valence electrons in the lowest five valence MOs and then we created single, double, triple, and quadruple excitations from the valence MOs of this reference function into the other eight valence orbitals. This process generated the 42 301 CSFs that we used in subsequent geometry optimization steps.

For the Al_3H C_{3v} structure, the MCSCF wave function was severely symmetry broken (for example, there were no pairs of degenerate molecular orbitals) which leads to unreliable geometrical displacements in the optimization. We were unable to repair or find a suitable MCSCF wave function; therefore, we optimized all of the Al_3H *minima* at the QCISD(T) level of theory in order to predict the lowest energy Al_3H structure, thus avoiding comparing energies at different levels of theory.

TABLE II. Correlated energies (a.u.) for the lowest doublet and quartet states of Al_3 at the respective MCSCF optimized geometries listed below.

	$^2A_1'$	$^2A_2''$	$^4A_2$	$^4B_1$
MCSCF	−725.787 81	−725.779 19	−725.776 45	−725.777 07
CCSD(T)	−725.886 43	−725.881 69	−725.880 74	−725.879 51
PMP4	−725.883 86	−725.877 66	−725.878 69	−725.877 63
QCISD(T)	−725.887 70	−725.882 20	−725.881 13	−725.879 85
R (Å)	2.57	2.66	2.65	2.78
θ (deg)	60.0	60.0	66.4	61.9

2. Higher level correlation energies

We used the general atomic and molecular electronic structure system (GAMESS)[16] computer program developed by M. Schmidt *et al.* to search the potential energy surfaces for minima and transition states at the MCSCF level of theory described above. Upon identifying such stationary points on the ground state surface, we then used the GAUSSIAN 92[17] suite of programs to calculate the QCISD(T), CCSD(T), and MP4 energies at these MCSCF stationary points to better quantify the various structure's relative energies. Unless otherwise specified, our *final* energy differences (i.e., dissociation energies and relative energies of stable isomers or transition states) are obtained from our QCISD(T) data, which we view as being our most accurate data.

III. FINDINGS

A. Al_3 energies and stable geometries

To achieve a feel for the accuracy of our calculations, we first optimized the geometries of the four lowest states ($^2A_1'$,$^2A_2''$,$^4A_2$,$^4B_1$) of the aluminum trimer at the MCSCF level and then calculated the relative energies of these four states at the several higher levels of theory discussed above. Our total energies and optimized geometries are shown in Table II.[20]

At our highest levels of theory, the σ-radical $^2A_1'$ state is predicted to lie lowest and the $^4B_1$ state to lie highest. However, the energy gap between these two states at the QCISD(T) level is only 5 kcal/mol. The relative energies of the two remaining low-lying states, the π-radical $^2A_2''$ and the $^4A_2$ states, vary depending on which correlation method one uses. The QCISD(T) and CCSD(T) methods predict the $^2A_2''$ state to lie slightly below the $^4A_2$ state; while the spin-projected MP4 results give the opposite ordering.

Based on the series of calculations whose results are presented here and Weltners experimental findings, we feel reasonably confident in concluding that the σ-radical $^2A_1'$ state is the ground state of Al_3 and that the $^4B_1$ state is the third excited state. The relative ordering of the π-radical $^2A_2''$ and $^4A_2$ states, both of which lie ca. 4 kcal/mol above the $^2A_1'$ state, is uncertain.

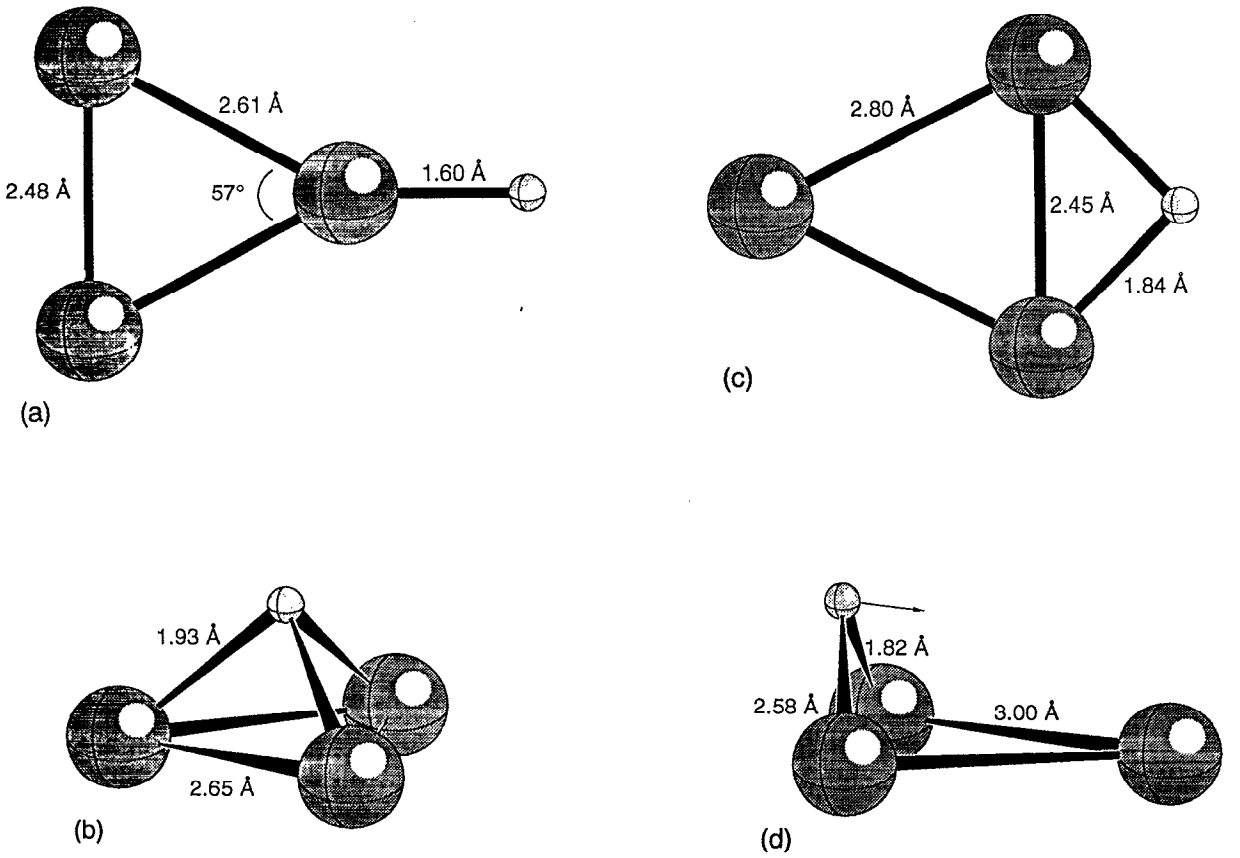

FIG. 3. (a) σ-bonded Al_3H structure. $\mu=0.22$ Debyes with $Al_3^-H^+$ character. (b) π-bonded Al_3H structure. $\mu=1.38$ Debyes with $Al_3^+H^-$ character. (c) Bridge-bonded Al_3H structure. $\mu=1.27$ Debyes with $Al_3^-H^+$ character. (d) False minimum Al_3H structure.

B. Al_3H stable geometries

1. C_{2v} structure

We found three low-energy minima on the ground state singlet Al_3H potential energy hypersurface using the MCSCF wave function detailed earlier. The first, shown in Fig. 3(a) involves a single σ-bond between the H atom and one of the Al atoms, and can be viewed as arising from simple coupling between the σ-radical $^2A_1'$ state of Al_3 and an H atom. The geometrical parameters and local harmonic vibrational frequencies of this structure are also shown in Fig. 3(a) and Table III, respectively, as are the zero-point energies (ZPE). The dipole moment of this structure is 0.22 Debyes, with the positive end of the dipole directed toward the H atom (i.e., it has $Al_3^-H^+$ character). In Table IV, the energy of this and other minima and transition states are given at the MCSCF and higher levels of correlation.

The Al–H bond strength of this species [i.e., D_e to form $^2A_1'$ Al_3 and H (^2S)] obtained from the QCISD(T) level of theory is 65 kcal/mol, which is comparable to Herzberg's[21] dissociation energy for diatomic AlH ($D_0^0<3.06$ eV=70.56 kcal/mol). Throughout this paper, all energy differences reported refer to nonzero-point corrected *electronic* energies, unless otherwise noted.

2. C_{3v} structure

A second low-energy singlet structure (of $^1A_1$ symmetry in the C_{3v} point group) was found at the MP2 level to have the geometry and vibrational frequencies detailed in Fig. 3(b) and Table III. This structure can be obtained via radical coupling of the Al_3 π-type $^2A_2''$ state with a ^2S hydrogen atom. This structure is predicted at the QCISD(T) level to have an

TABLE III. Local harmonic vibrational frequencies (cm^{-1}) for Al_3H structures.

σ-bonded[a]	π-bonded[b]	C_{2v}-bridge bonded[a]
269	195 E	159
316	195 E	188
367	332A_1	240
388	955 E	342
438	955 E	780
1761	1041A_1	1151
ZPE=5.06 kcal/mol	ZPE=5.25 kcal/mol	ZPE=4.09 kcal/mol

[a]MCSCF frequencies.
[b]MP2 frequencies.

TABLE IV. Total energies for Al_3H structures using various methods. Energies are in a.u.

	C_{3v} π-bonded	C_{2v} σ-bonded	Planar: bridge-bonded	C_{3v}–C_{2v} TS	C_{3v}–C_{3v} TS
MCSCF	See text	−726.383 59	−726.348 38	−726.353 35	−726.351 59
MP2	−726.439 43	−726.446 75	−726.413 79	−726.408 26	−726.414 85
MP3	−726.469 95	−726.471 61	−726.445 74	−726.443 50	−726.446 27
MP4	−726.487 73	−726.490 12	−726.464 22	−726.460 24	−726.466 98
CCSD(T)	−726.490 81	−726.490 68	−726.466 21	−726.466 25	−726.468 13
QCISD(T)	−726.491 31	−726.491 23	−726.466 81	−726.466 85	−726.468 84

Hydrogen atom $E=-0.499\ 33$
Al_3H false minimum QCISD(T) energy $=-726.477\ 018\ 56$

electronic energy only 0.05 kcal/mol below the C_{2v} σ-bonded structure mentioned above, as a result of which we conclude that the actual lowest energy Al_3H structure cannot be reliably predicted at the level of theory performed here. This C_{3v} structure has a dipole moment of 1.38 Debye, displaying significant $Al_3^+H^-$ character, opposite that of the C_{2v} structure.

3. Planar structure

The third low-energy structure found in our MCSCF calculations for Al_3H is of $^1A_1$ symmetry in the C_{2v} point group and has the planar geometry and vibrational frequencies detailed in Fig. 3(c) and Table III. This bridge-bonded structure has three low frequency vibrations, lies only 15 kcal/mol above the σ-bonded C_{2v} structure at the QCISD(T) level of theory, and has a dipole moment of 1.27 Debyes with the positive end of the dipole directed towards the H atom.

4. A false minimum

Another Al_3H structure that merits mention is the three-center bridge-bonded structure shown in Fig. 3(d) which lies 9 kcal/mol above the C_{2v} σ-bonded structure. The SCF-level vibrational analysis showed this to be a local minimum at the geometry shown. However, when MP2 and MCSCF calculations were performed, negative curvature along the a' mode shown in Fig. 3(d) was obtained, and further geometry optimization produced the above mentioned C_{3v} π-bonded structure.

This dramatic change in surface curvature is due to second order Jahn–Teller (SOJT) effects. At the SCF level, the lowest excited state capable of coupling to the singlet ground state to produce negative curvature along a direction connecting this bridge-bonded structure and the C_{3v} structure is 120 kcal/mol above the ground state. However, at the CI level, this state drops to only 18 kcal/mol above the ground state; as a result SOJT instability occurs.

C. Interconversions among stable geometries of Al_3H

Transition states (TSs) connecting the most stable geometries described above were also located and are characterized by their geometries, energies, and local harmonic imaginary vibrational frequencies detailed in Fig. 4 and Table V.

The reaction path connecting the π-bonded C_{3v} structure to the σ-bonded C_{2v} structure is pictured in Fig. 4(a) with the geometries and other characteristics for the corresponding C_s symmetry TS. This TS lies 15 kcal/mol above the σ-bonded structure at the QCISD(T) level of theory, and the imaginary frequency is 365 cm^{-1}. The height of this barrier and the width characterized by the small imaginary frequency make tunneling between the C_{2v} and C_{3v} structures very improbable.

In Fig. 4(b) we describe the reaction path connecting pairs of equivalent π-bonded C_{3v} structures passing through a TS having C_{2v} symmetry. Along this path, which has a barrier of 14 kcal/mol at the QCISD(T) level of theory, the H atom moves from one side of the plane formed by the three Al atoms to the other, preserving one σ_v symmetry plane throughout. Again the barrier and small imaginary frequency (393 cm^{-1}) preclude significant tunneling.

D. Possible D_{3h} structure for Al_3H

We also examined the possibility that a D_{3h} structure with the H atom at the center of an equilateral Al_3 moiety could be either geometrically stable or a first-order transition state. However, we found that the lowest electronic state for such a constrained structure possessed distortions with negative curvatures of E and A_1 symmetries. Hence, we predict that no such D_{3h} Al_3H minimum or transition state structure is possible.

TABLE V. Local MCSCF harmonic vibrational frequencies (cm^{-1}) for Al_3H transition state structures.

C_{3v}–C_{3v}	C_{3v}–C_{2v}
393i	365i
186	161
251	186
254	257
965	302
1489	1555
ZPE=4.47 kcal/mol	ZPE=3.52 kcal/mol

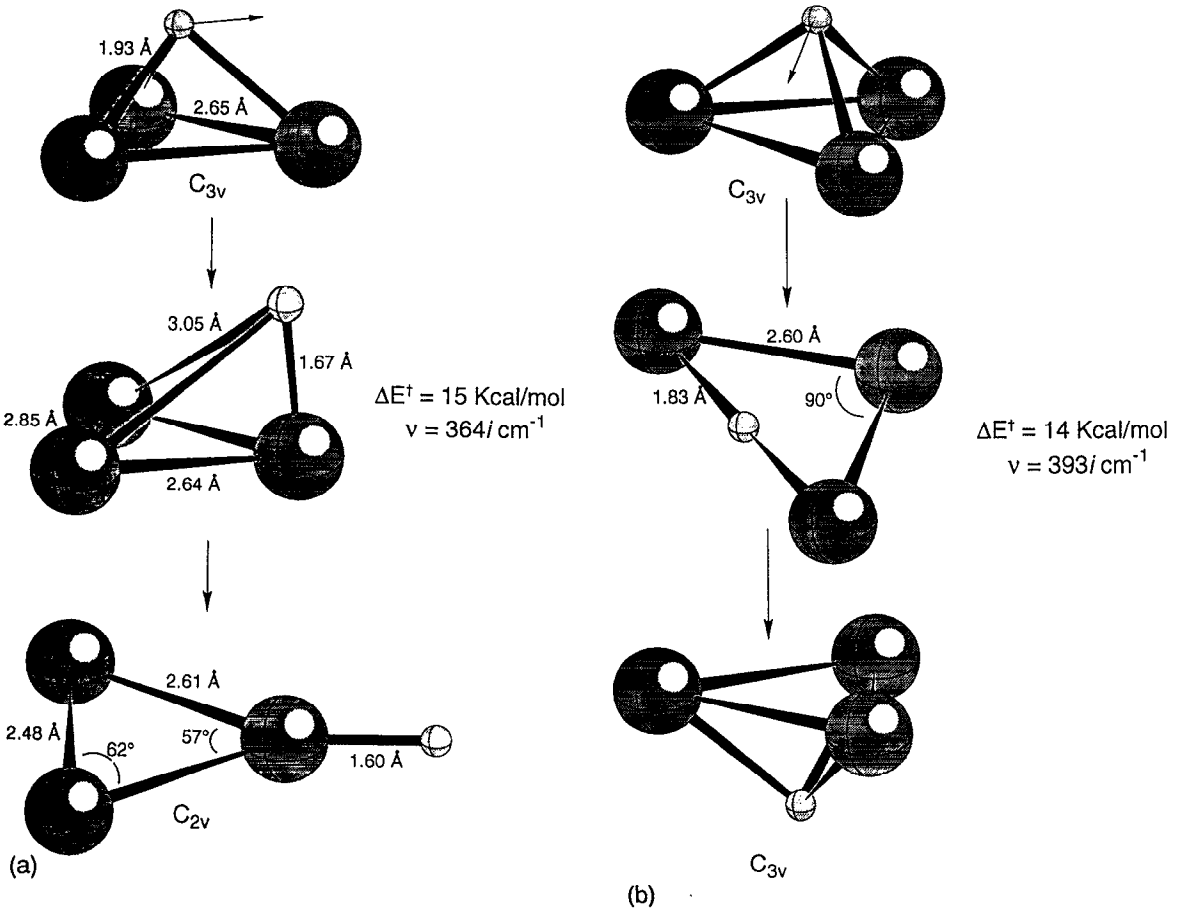

FIG. 4. (a) Al_3H C_{3v} to C_{2v} reaction path. (b) Al_3H C_{3v} to C_{3v} reaction path.

E. Other transition states

Although we were able to identify TSs connecting C_{3v} to C_{2v} and C_{3v} to C_{3v} structures (all on the ground state surface), we were unable to find (i) any transition state connecting to the planer structure or (ii) a TS connecting C_{2v} to C_{2v}.

IV. SUMMARY

We located three local minima and two first-order transition states on the Al_3H potential energy surface. We found that two of the Al_3H minima are very close in energy ($\Delta E = 0.05$ kcal/mol) with the third lying 15 kcal/mol above the others. One of the two transition states connects a C_{2v} minimum to a C_{3v} minimum with a barrier of 15 kcal/mol, and the other TS connects equivalent C_{3v} minima with a barrier of 14 kcal/mol. We also calculated and compared the four lowest electronic states of Al_3 (i.e., the $^2A_1'$, $^2A_2''$, $^4A_2$, and $^4B_1$ states). We predict the $^2A_1'$ state, with the valence orbital occupancy of $(a_1')^2(e')^4(a_2'')^2(a_1')^1$, to be the ground state. The $^4B_1$ state is the highest in energy of those studied because it is a first order saddle point on the upper surface of the double cone. The ordering of the intermediate $^2A_2''$ and $^4A_2$ states is still uncertain.

ACKNOWLEDGMENT

This work was supported by the Office of Naval Research and The National Science Foundation, Grant No. CHE-9116286.

[1] (a) J. Koutecky and P. Fantucci, Chem. Rev. **86**, 539 (1986); (b) M. Morse, *ibid.* **86**, 1049 (1986); (c) M. Mandich, W. Reent, and V. Bondybey, in *Atomic and Molecular Clusters*, edited by E. Bernstein (Elsevier Science, Amsterdam, 1990); (d) A. Castleman and R. Keesee, Chem. Rev. **86**, 589 (1986); (e) T. Upton, Phys. Rev. Lett. **56**, 2186 (1986); (f) T. Upton, D. Cox, and A. Kaldor, *Physics and Chemistry of Small Clusters*, NATO ASI SERIES, (Plenum, New York, 1987), Vol. 158; (g) A. Boldyrev and P. von R. Schleyer, J. Am. Chem. Soc. **113**, 9045 (1991).

[2] (a) B. Rao, Phys. Rev. B **32**, 2058 (1985); (b) D. Davies and D. Del Conde, Faraday Discuss. Chem. Soc. **55**, 369 (1973); (c) Chem. Phys. **12**, 45 (1976); (d) R. Whiteside, R. Krishan, J. Pople, M. Krogh-Jesperson, P. von R. Schleyer, and G. Wenke, J. Comp. Chem. **1**, 307 (1980); (e) R. Brewington, C. Bender, and H. Schaefer III, J. Chem. Phys. **64**, 905 (1976); (f) G. Pacchioni and J. Koutecky, *ibid.* **77**, 5850 (1982); (g) J. Daudey, O. Novaro, W. Kolos, and M. Berrondo, *ibid.* **71**, 4297 (1979); (h) J. Gole, R. Childs, D. Dixon, and R. Eades, *ibid.* **72**, 6369 (1980); (i) A. Companion, D. Steible, and A. Starshak, *ibid.* **49**, 3637 (1968); (j) J. Flad, H. Stoll, and H. Preuss, *ibid.* **71**, 3042 (1979).

[3] (a) H. Jahn and E. Teller, Proc. R. Soc. London, Ser. A, **161**, 220 (1937); (b) R. Englman, *The Jahn Teller Effect in Molecules and Crystals* (Wiley-Interscience, New York, 1972); (c) I. Bersuker, *The Jahn-Teller Effects and Vibronic Interactions in Modern Chemistry* (Plenum, New York, 1984); (d) Ph. Dugourd, J. Chevaleyre, J. Perrot, and M. Broyer, J. Chem.

Phys. **93**, 2332 (1990); (e) J. Martins, R. Car, and J. Buttet, *ibid.* **78**, 5646 (1983); (f) W. Gerber and E. Schumacher, *ibid.* **69**, 1692 (1978); (g) T. Thompson and A. Mead, *ibid.* **82**, 2408 (1985); (h) T. Thompson, D. Truhlar, and A. Mead, *ibid.* **82**, 2392 (1985); (i) M. Gutowski and J. Simons, *ibid.* **100**, 1308 (1994); (j) **101**, 4867 (1994); (k) in J. Chem. Phys. to be published.

[4] R. Hernandez and J. Simons, J. Chem. Phys. **94**, 2961 (1991).

[5] R. Hernandez and J. Simons, J. Chem. Phys. **96**, 8251 (1992).

[6] Y. Hamrick, R. Van Zee, and W. Weltner, J. Phys. Chem. **96**, 1767 (1992).

[7] D. Cox, D. Trevor, R. Whetten, E. Rohlfing, and A. Kaldor, J. Chem. Phys. **84**, 4651 (1986).

[8] (a) J. Tse, J. Chem. Phys. **92**, 2488 (1990); (b) J. Mol. Struct. **165**, 21 (1988); (c) C. Bauschlicher and L. Pettersson, J. Chem. Phys. **87**, 2198 (1987); (d) G. Pacchioni, P. Fantucci, and J. Koutecky, Chem. Phys. Lett. **142**, 85 (1987); (e) H. Basch, *ibid.* **136**, 289 (1987).

[9] C. Bauschlicher, L. Pettersson, and T. Halicioglu, J. Chem. Phys. **87**, 2205 (1987).

[10] Z. Fu, G. Lemire, Y. Hamrick, S. Taylor, J. Shui, and M. Morse, J. Chem. Phys. **88**, 3524 (1988).

[11] D. E. Woon and T. H. Dunning, Jr., J. Chem. Phys. **98**, 1358 (1993).

[12] P. J. Hay and W. R. Wadt, J. Chem. Phys. **82**, 270 (1985).

[13] A. Schafer, H. Horn, and R. Ahlrichs, J. Chem. Phys. **97**, 2571 (1992).

[14] Unpublished Dunning-VTZ basis set.

[15] (a) R. Krishnan, J. S. Binkley, R. Seeger, and J. A. Pople, J. Chem. Phys. **72**, 650 (1980); (b) M. J. Frisch, J. A. Pople, and J. S. Binkley, *ibid.* **80**, 3265 (1984); (c) T. Clark, J. Chandrasekhar, G. W. Spitznagel, and P. v. R. Schleyer, J. Comput. Chem. **4**, 294 (1983); (d) A. D. McLean and G. S. Chandler, J. Chem. Phys. **72**, 5639 (1980).

[16] M. W. Schmidt, K. K. Baldridge, J. A. Boatz, S. T. Elbert, M. S. Gordon, J. H. Jensen, S. Koseki, N. Matsunaga, K. A. Nguyen, S. Su, T. L. Windus, M. Dupuis, and J. A. Montgomery, Jr., J. Comp. Chem. **14**, 1347 (1993).

[17] GAUSSIAN 92, Revision C, M. J. Frisch, G. W. Trucks, M. Head-Gordon, P. M. Gill, M. W. Wong, J. B. Foresman, B. G. Johnson, H. B. Schlegel, M. A. Robb, E. S. Replogle, R. Gomperts, J. L. Andres, K. Raghavachari, S. Binkley, C. Gonzalez, R. L. Martin, D. J. Fox, D. J. DeFrees, J. Baker, J. J. P. Stewart and J. A. Pople (Gaussian Inc., Pittsburgh, PA, 1990).

[18] C. E. Moore, *Tables of Atomic Energy Levels* (U.S. Govt. Printing Office, Washington, D.C., 1971).

[19] W. C. Lineberger and H. Hotop, J. Phys. Chem. Ref. Data **14**, 731 (1985).

[20] For Al_3 we chose to optimize the geometry using the MCSCF method with all 9 valence electrons in the 12 valence orbitals using C_{2v} spacial symmetry to constrain the nuclei and also in constructing the CSFs. This method generated 37 928 CSFs for the quartet states and 25 723 CSFs for the doublet states. The C_{2v} optimization was closely monitored and corrected when necessary to maintain D_{3h} symmetry. QCISD(T), CCSD(T), and PMP4 calculations were then performed at the MCSCF stationary points to better quantify the relative energies.

[21] G. Herzberg, *Molecular Spectra & Molecular Structure vol I-Spectra of Diatomic Molecules* (Van Nostrand Reinhold, New York, 1950).